Pergamon

Biochemical Pharmacology, Vol. 48, No. 6, pp. 1289–1296, 1994.

0006-2952/94 $7.00 + 0.00

0006-2952(94)E0184-M

EFFECT OF PHOSPHOLIPID HYDROLYSIS BY PHOSPHOLIPASE A_2 ON THE KINETICS OF ANTAGONIST BINDING TO CARDIAC MUSCARINIC RECEPTORS

BERNHARD RAUCH,* FERAYDOON NIROOMAND, FRANK C. MESSINEO,†
ANGELIKA WEIS, WOLFGANG KÜBLER and WILHELM HASSELBACH‡

Abteilung Innere Medizin III, Medizinische Klinik, Universität Heidelberg, Bergheimerstr. 58, 69115 Heidelberg, F.R.G.; †Division of Cardiology, Department of Medicine, University of Connecticut Health Center, Farmington, CT 06032, U.S.A.; and ‡Max-Planck-Institut für medizinische Forschung, Jahnstr. 29, 69120 Heidelberg, F.R.G.

(*Received* 8 *July* 1993; *accepted* 12 *April* 1994)

Abstract—Activation of phospholipases during prolonged myocardial ischemia could contribute to the functional derangement of myocardial cells by altering the phospholipid environment of a number of membrane bound proteins including receptors. The present study examined the kinetics of muscarinic receptor antagonist [^{3}H]quinuclidinyl benzilate binding ([^{3}H]QNB) to muscarinic receptors of highly purified sarcolemmal membranes under control conditions and after treatment with phospholipase A_2 (PLA_2; EC 3.1.1.4.). Initial binding rates of QNB exhibited saturation kinetics, when plotted against the ligand concentration in control and PLA_2 treated sarcolemmal membranes. This kinetic behaviour of QNB-binding is consistent with at least a two step binding mechanism. According to this two step binding hypothesis an unstable intermediate receptor–QNB complex (R*QNB) forms rapidly, and this form undergoes a slow conversion to the high affinity ligand–receptor complex R-QNB. The Michaelis constant K_m of R-QNB formation was 1.8 nM, whereas the dissociation constant K_d obtained from equilibrium measurements was 0.062 nM. After 5 min exposure of sarcolemmal membranes to PLA_2 QNB binding capacity (B_{max}) was reduced by 62%, and the affinity of the remaining receptor sites was decreased by 47% ($K_d = 0.116$ nM). This PLA_2-induced increase of K_d was accompanied by a corresponding increase of K_m, whereas the rate constants k_2 and k_{-2} of the hypothetical slow conversion step (second reaction step) remained unchanged. These results suggest that binding of QNB to cardiac muscarinic receptors induces a transition in the receptor–ligand configuration, which is necessary for the formation of the final high affinity R-QNB complex. PLA_2-induced changes of the lipid environment result in the inability of a part of the receptor population to undergo this transition, thereby inhibiting high affinity QNB-binding.

Key words: cardiac muscarinic receptors; phospholipase A_2; sarcolemma; quinuclidinyl benzilate; antagonist binding; binding kinetics

Muscarinic receptors of brain and heart tissue are sensitive to changes in their lipid environment [1–6]. Therefore, increased phospholipase activity, as has been suggested to occur during prolonged myocardial ischemia [7–13], may interfere with the normal function of the cardiac muscarinic receptor system. Recent studies have shown that phospholipase induced hydrolysis of membrane phospholipids reversibly reduced the number of sarcolemmal muscarinic receptors identified by [^{3}H]QNB§ binding, and also decreased the affinity of the remaining receptors [5, 6]. As these results and those of others suggest, that [^{3}H]QNB binding to muscarinic receptors may not follow a simple bimolecular mechanism [14, 15], we examined this possibility further by measuring the effect of PLA_2 treatment of sarcolemmal membranes on the initial rate kinetics of [^{3}H]QNB-binding. The present data support the hypothesis that QNB-binding to sarcolemmal membranes follows at least a two step mechanism where the rapid formation of an unstable intermediate is followed by its slow conversion to a stable ligand–receptor complex. Membrane phospholipid hydrolysis by PLA_2 inhibits QNB-binding in part by preventing the slow conversion to the stable QNB–receptor complex.

* Corresponding author. Tel. 0049-7681-29150; FAX 0049-7681-29144.

§ Abbreviations: QNB, quinuclidinyl benzilate; PLA_2, phospholipase A_2; K_m, Michaelis constant; B_{max}, maximal binding under equilibrium conditions; R, receptor; R_0, total concentration of the receptor; R*QNB, unstable receptor–QNB complex; R-QNB, stable receptor–QNB complex; K_d, overall dissociation constant measured under equilibrium conditions; K_1, dissociation constant of step one; k_2 and k_{-2}, rate constants of step two; V_{max}, maximal initial association rate; v_0, apparent initial association rate at a definite QNB-concentration.

MATERIALS AND METHODS

Preparation of sarcolemmal vesicles. Highly purified sarcolemmal vesicles were prepared from

canine cardiac ventricles according to the method of Jones *et al.* [16] with slight modifications [17]. This preparation has been characterized previously, and it is comprised of predominantly sealed right-side out membrane vesicles [17]. Protein was determined according to Lowry *et al.* [18].

Treatment of sarcolemmal vesicles with PLA_2. Bee venom PLA_2 (phosphatide-2-acyl-hydrolase; EC 3.1.1.4) was purchased from the Sigma Chemical Co. (St Louis, MO, U.S.A.). This PLA_2 is known to be of high purity and free of mellitin [19]. PLA_2 was stored at −20° in a stock solution (100 U PLA_2/mL) containing 50 mM Tris–HCl (pH 7.4), 5 mM $CaCl_2$, and 50% glycerol (buffer I). Under these conditions PLA_2 activity can be retained for at least 1 year [19]. Ten microliters PLA_2 in buffer I were added to 1 mL sarcolemmal vesicles (400 μg/mL) suspended in 10 mM $NaHCO_3$, 20 mM HEPES (pH 7.4, 25°; buffer II). Control experiments were performed in the same way but without PLA_2 in buffer I. After 5 min of incubation the reaction was stopped by dilution with 20 mL ice-cold buffer II. Treated sarcolemmal membranes then were separated from buffer by two 30 min centrifugations at 100,000 *g*. Protein recovery after this treatment was greater than 85% in control and PLA_2 treated membranes. Under these conditions a 5 min exposure of sarcolemmal membranes to PLA_2 results in hydrolysis of approximately 30% of the total phospholipid pool [5].

[^{3}H]QNB-binding assay. Equilibrium binding was determined by incubation of [^{3}H]QNB (30–600 pM) with 10–15 μg sarcolemmal protein for 120 min at 25° in a 5 mL reaction mixture containing 5 mM $MgCl_2$, 20 mM Tris–HCl (pH 7.4), and 5 mM NaH_2PO_4 (buffer III). Binding reactions were terminated by rapid filtration through Whatmann GF/B filters using a Brandel Cell Harvester (Gaithersburg, MD, U.S.A.). Filters were washed four times with 5 mL of 50 mM Tris–HCl (pH 7.4), and placed in 4 mL Biofluor. Radioactivity was determined by liquid scintillation spectroscopy (Delta 300, Searle Analytic Inc., Des Plaines, IL, U.S.A.). Specific binding was determined from the difference in [^{3}H]QNB bound in the absence and presence of 1 μM atropine sulfate.

The complete time course of [^{3}H]QNB receptor association was measured by adding sarcolemmal membranes (final protein concentration: 2 μg/mL) to buffer III that contained 60, 150 or 600 pM [^{3}H]-QNB. At selected time intervals (0.5–90 min), aliquots of 5 mL of the reaction mixture were filtered through Whatmann GF/B filters mounted on Millipore vacuum manifolds (Millipore Corp., Bedford, MA, U.S.A.). The filters were washed with 20 mL 50 mM Tris–HCl (pH 7.4), and radioactivity was determined as described above. Under these experimental conditions only the stable, high affinity [^{3}H]QNB–receptor complex can be measured, and the formation of this stable receptor–[^{3}H]QNB complex is slow [5, 6, 14, 15; Fig. 1]. Apparent initial rates of [^{3}H]QNB association therefore can be estimated without using rapid mixing devices by taking aliquots for filtration 0.0, 0.5, 1.0, 1.5, 3.0 and 6.0 min after starting the reaction. Apparent linearity of [^{3}H]QNB association was observed between the time points zero, 0.5, and 1.0 min using [^{3}H]QNB concentrations between 60 pM and 2400 pM.

Calculations. Maximal binding of [^{3}H]QNB at equilibrium conditions (B_{max}) and the dissociation constant (K_d) were determined by double reciprocal plots of [^{3}H]QNB binding isotherms (Fig. 4B). Maximal binding velocity (V_{max}) and the Michaelis constant (K_m) were determined from analysis of double reciprocal plots of the initial binding rates (v_0) versus [^{3}H]QNB concentration (Fig. 3B).

Assuming a two step binding mechanism the individual dissociation constants ($K_1 \approx K_m$; $K_2 = k_{-2}/k_2$) and the rate constants of the second step (k_2 and k_{-2}) were estimated from the equilibrium measurements and the initial rate kinetics as described in the Appendix.

Materials. All chemicals were reagent grade. L[^{3}H]QNB and Biofluor were obtained from New England Nuclear (Boston, MA, U.S.A.). Atropine sulfate was purchased from the Sigma Chemical Co. (St Louis, MO, U.S.A.).

RESULTS

Initial rate kinetics of [^{3}H]QNB-binding

[^{3}H]QNB-association exhibited a monoexponential time course at control conditions and after PLA_2 treatment (Figs 1A,B; 2A,B). Under control conditions and after PLA_2 treatment, binding equilibrium was reached about 90 min after the start of the reaction (Figs 1A, 2A).

The initial rates of [^{3}H]QNB-binding were estimated as described in Materials and Methods. The dependence of these apparent initial rates on total [^{3}H]QNB concentration exhibited saturation kinetics both under control conditions and after PLA_2 treatment (Fig. 3A). The apparent maximal velocities of [^{3}H]QNB-association V_{max}, the Michaelis constants K_m obtained from the corresponding double reciprocal plots (Fig. 3B), as well as the calculated rate constants of the conversion step k_2 and k_{-2} are summarized in Table 1.

QNB-binding under equilibrium conditions

[^{3}H]QNB-binding to canine sarcolemmal membranes measured under equilibrium conditions could be characterized by a single class of binding sites both under control conditions and after PLA_2 treatment. Under control conditions Scatchard analysis of [^{3}H]QNB-binding revealed a B_{max} of 5.8 ± 1.0 pmol/mg and K_d of 62 ± 14 pM. After PLA_2 treatment of sarcolemmal membranes, B_{max} was reduced to 2.2 ± 0.5 pmol/mg and K_d increased to 116 ± 19 pM (N = 4; Fig. 4A,B). These data are similar to results reported previously [5, 6].

DISCUSSION

The saturation kinetics of the initial rates of [^{3}H]-QNB-binding as demonstrated in the present study (see Fig. 3A) exclude a simple bimolecular binding

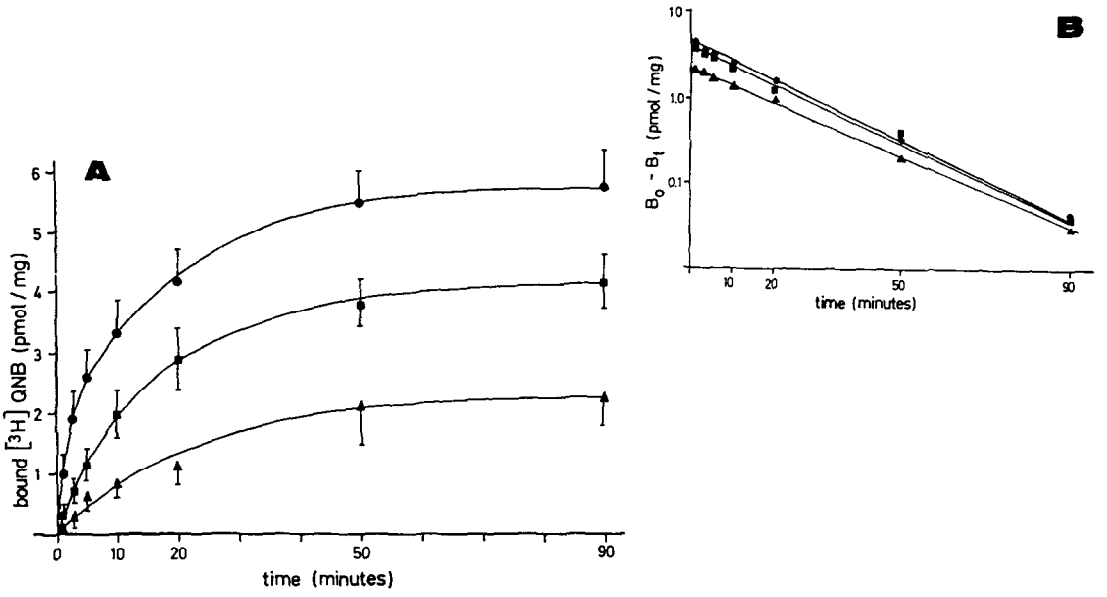

Fig. 1. [^{3}H]QNB association under control conditions using 60 pM (▲), 150 pM (■), and 600 pM (●) [^{3}H]QNB (A). The monophasic time course of [^{3}H]QNB association is demonstrated by the corresponding linear semilogarithmic plots (B). Details of the experimental conditions are described in Materials and Methods. Values are means ± SD of N = 4.

reaction, since a bimolecular binding mechanism

$$R + QNB \underset{k_{-1}}{\overset{k_1}{\rightleftharpoons}} R{-}QNB$$

would result in an initial association rate that linearly depends on the free concentration of the ligand. Therefore, the simplest reaction model to assume is a two step binding mechanism:

$$R + QNB \underset{k_{-1}}{\overset{k_1}{\rightleftharpoons}} R^*QNB \underset{k_{-2}}{\overset{k_2}{\rightleftharpoons}} R{-}QNB.$$

(step 1) (step 2)

According to Michaelis–Menten this reaction model includes the rapid formation of an unstable

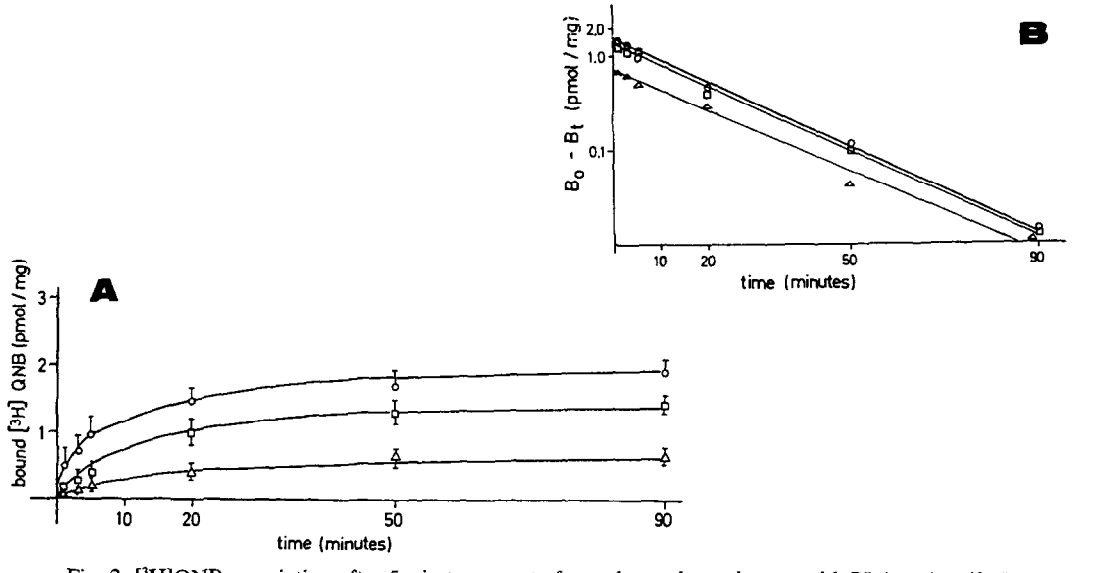

Fig. 2. [^{3}H]QNB association after 5 min treatment of sarcolemmal membranes with PLA_2 using 60 pM (△), 150 pM (□), and 600 pM (○) [^{3}H]QNB (A). The monophasic time course of [^{3}H]QNB association is demonstrated by the corresponding linear semilogarithmic plots (B). Details of the experimental conditions are described in Materials and Methods. Values are means ± SD of N = 4.

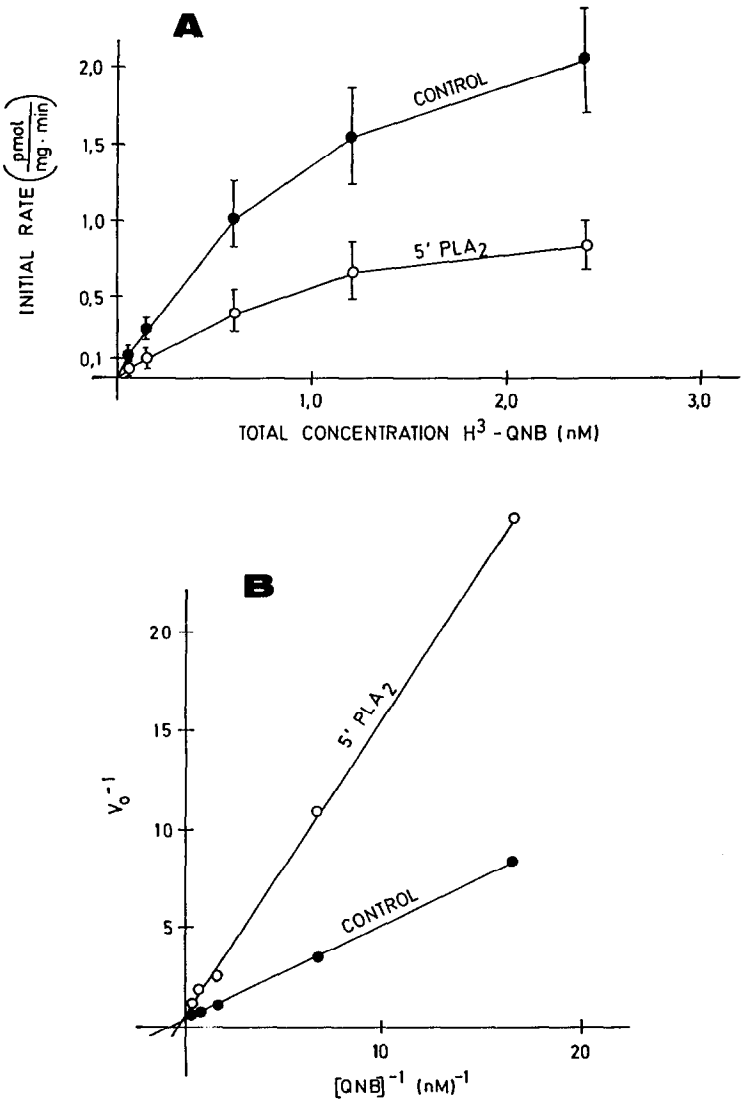

Fig. 3. Dependence of the apparent initial [^{3}H]QNB binding rate on [^{3}H]QNB concentration (A: control conditions = black symbols; 5 min PLA_2 = white symbols). The Michaelis constant K_m and the apparent maximal [^{3}H]QNB association rate was estimated from the corresponding double reciprocal plots $1/v_0$ versus 1/[^{3}H]QNB (B). Details of the experimental conditions are described in Materials and Methods. Values are means ± SD of N = 6.

intermediate R*QNB that is followed by a much slower conversion to the final high affinity complex R-QNB. The monophasic time course of [^{3}H]QNB association (Figs 1B,2B) suggests that under the present experimental conditions only the final high affinity ligand receptor complex R-QNB, but not the intermediate R*QNB, is measured. A rapid dissociation of the intermediate R*QNB during the washing and filtering procedures would be in accordance with the assumption of a high rate constant k_{-1}, which however cannot be determined from the available data. Similar binding mechanisms, as suggested here, are known from sequences of some enzyme reactions like the phosphorylation of sarcoplasmic reticulum calcium ATPase by inorganic phosphate [20].

Assuming the formation of the intermediate R*QNB (step 1) is much faster than its conversion to R-QNB (step 2), the initial binding rates (v_0) are related to the concentration of QNB, as described by the following equation (see Appendix eqn 2a; see also Fig. 3B):

$$\frac{1}{v_0} = \frac{1}{k_2[R_0]} + \frac{K_m}{k_2[R_0]} \cdot \frac{1}{[QNB]}.$$

In this equation $[R_0]$ is the total concentration of the receptor, which has been estimated by the measurement of maximal binding of [^{3}H]QNB (B_{max}, see Fig. 4). The QNB concentration needed for reaching the half maximal binding velocity is described by the Michaelis constant K_m, as obtained

Table 1. Kinetic parameters of [^{3}H]QNB-binding to sarcolemmal membranes

	Control	5 min PLA_2
K_d (M)	6.2×10^{-11}	11.6×10^{-11}
K_1 (M)	1.8×10^{-9}	3.45×10^{-9}
k_2 (sec^{-1})	0.014	0.015
k_{-2} (sec^{-1})	5.0×10^{-4}	5.2×10^{-4}
V_{max} (mol/mg/min)	5.0×10^{-12}	2.0×10^{-12}
B_{max} (mol/mg)	5.8×10^{-12}	2.2×10^{-12}

K_d = dissociation constant obtained from Scatchard analysis of QNB-binding as measured under equilibrium conditions. K_1 = dissociation constant of the first binding step that forms the unstable intermediate R*QNB. K_1 can be approximated by the Michaelis constant K_m that is obtained from the analysis of the double reciprocal plots of the initial binding rates versus QNB concentration. k_2, k_{-2} = rate constants of the slow conversion step (step 2 of the binding reaction). V_{max}= maximal initial association rate. B_{max}= maximal binding determined under equilibrium conditions.

from the x-intercepts of the double reciprocal plots $1/v_0$ versus $1/[^3H]QNB$ (Fig. 3B; Table 1). As the conversion of the unstable intermediate complex R*QNB to the stable complex R-QNB is rate limiting (step 2), the initial rate v_0 equals the product of the rate constant k_2 of the second step and the concentration of the intermediate complex R*QNB (see Appendix, eqn 1). Maximal velocity of QNB-binding then can be obtained by extrapolating the concentration of QNB to infinite values (see double reciprocal plot in Fig. 3B). Under these conditions all receptor binding sites are occupied by QNB, and the amount of R*QNB equals R_0, which can be estimated by measuring B_{max}. The rate constant k_2 can then be estimated by the following equation (see Appendix, eqn 1b):

$$k_2 = V_{max}/R_0.$$

The rate constant k_{-2} which describes the rate limiting step of the dissociation of the stable ligand receptor complex R-QNB, now can be obtained (a) from the analysis of QNB-binding under equilibrium conditions and (b) from the corresponding steady state equation (see Appendix, eqn 6):

$$\frac{1}{[\text{R-QNB}]} = \frac{k_{-2} + k_2}{k_2} \cdot \frac{1}{[R_0]} + \frac{k_{-2}K_1}{k_2[R_0]} \cdot \frac{1}{[\text{QNB}]}.$$

This equation describes double reciprocal plots of the saturation isotherms of bound [^{3}H]QNB versus free [^{3}H]QNB under equilibrium conditions (Fig. 4B). In this Figure the x-intercepts represent the negative reciprocal values of the dissociation constants K_d that are also defined by the quotient between y-intercept and the slope of the linear curves (Fig. 4B; see Appendix, eqn 7a):

$$K_d = K_1 \cdot \frac{k_{-2}}{k_{-2} + k_2}.$$

This equation allows the calculation of the rate constant k_{-2} as the values of K_d, K_1, and k_2 are known (see above considerations). The kinetic constants of [^{3}H]QNB binding derived from the experimental data and the calculations described above are summarized in Table 1. Due to the slow reverse transition step (k_{-2}) these data show that the QNB-concentration needed for reaching half maximal velocity of [^{3}H]QNB association is more than one order of magnitude greater than the concentration needed for half maximal QNB-equilibrium binding.

The assumption that the antagonist QNB induced a conversion of the muscarinic receptor agrees with earlier results obtained in developing chick hearts and porcine atrial muscarinic receptors [14, 15]. The potential of ligands to influence receptor conformational states is also consistent with the hypothesis that antagonist occupied receptors bind more tightly to inactive forms of G-proteins [21, 22]. According to this hypothesis binding of QNB would not only occlude the ligand-binding site and thereby prevent agonists from acting, but also induce a conversion of the muscarinic receptor to a conformation that preferably binds to inactive forms of inhibitory G-proteins, like the GDP–G_i complex.

One effect of phospholipid hydrolysis by PLA_2 on muscarinic receptor antagonist binding is the reduction of B_{max}. In terms of the hypothetical reaction model described above, PLA_2 treatment may convert a part of the available receptors resulting in the inability of these receptors to form the stable R-QNB complex. However, the kinetics of the slow conversion step (step 2) of the remaining receptor sites were unaltered. Their reduced affinity, as described by the overall dissociation constant K_d, therefore is solely due to the increase in the dissociation constant of the first rapid step K_1 (see Table 1).

The effect of PLA_2 on [^{3}H]QNB-binding resembles a "linear mixed type inhibition" [23] that can be described by the following hypothetical reaction scheme:

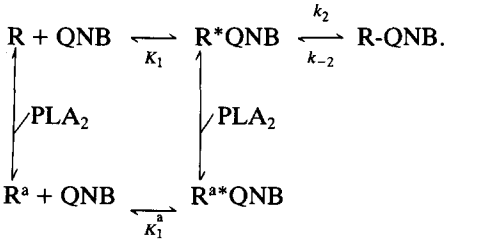

According to this reaction scheme phospholipid hydrolysis by PLA_2 leads to a conversion of a part of the receptor population R to R^a. PLA_2 induced conversion may also involve the unstable intermediate R*QNB. Although with lower affinity, as described by the dissociation constant K_1, the receptor population R^a may still be able to interact with QNB to form an unstable intermediate R^a*QNB. However, R^a*QNB is not able to directly convert to a stable high affinity complex between the receptor and QNB, forming R^a-QNB. In the presence of PLA_2 therefore, some of the available receptor population will always be in the non-productive R^a*QNB form, thereby reducing maximal

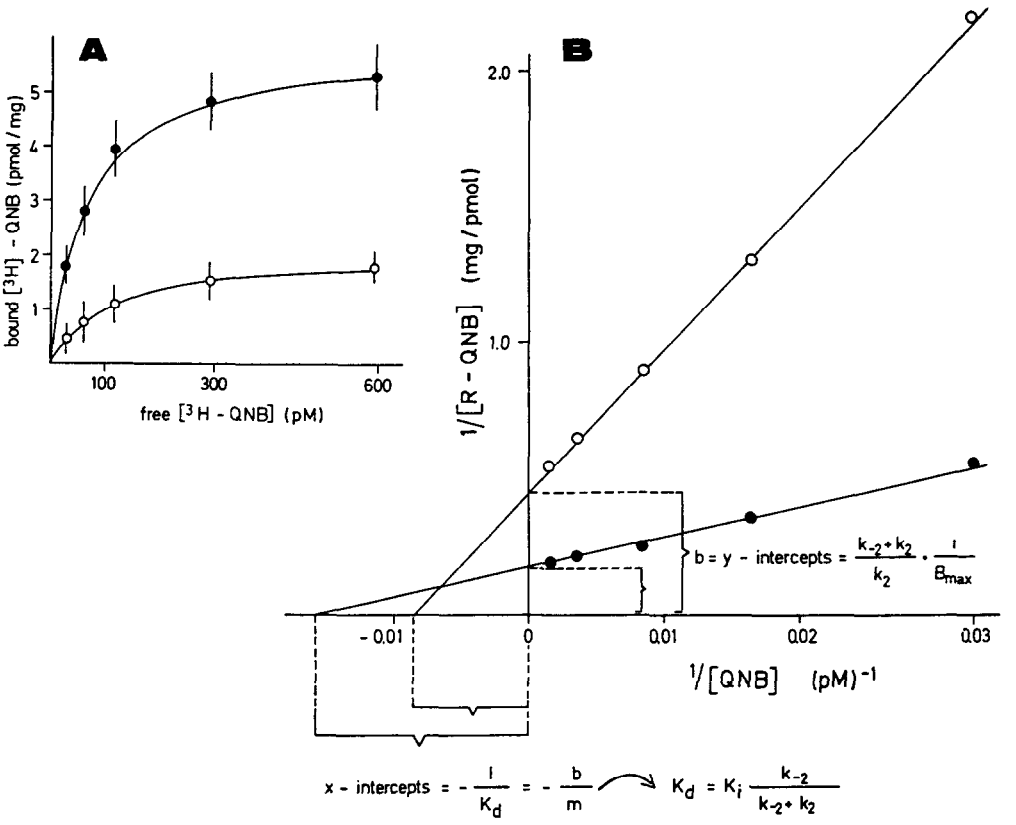

Fig. 4. Dependence of [^{3}H]QNB binding at equilibrium conditions on the free concentration of [^{3}H]-QNB (A: control conditions = black symbols; 5 min PLA_2= white symbols). The saturation isotherms were converted to double reciprocal plots 1/bound [^{3}H]QNB versus 1/free [^{3}H]QNB (B). K_d was estimated from the x-intercepts, which correspond to the quotient between the slope (m) and the y-intercepts (b). From the equation $K_d = m/b$ the rate constant k_{-2} was calculated as outlined in Discussion (for mathematical details see also Appendix). Values are means ± SD of N = 4.

binding (B_{max}) but also maximal association rate (V_{max}). Furthermore, a portion of the receptor population will always exist in the lower affinity R^a form, thereby reducing overall affinity K_d (see Table 1).

In summary, the present results support the concept that antagonist binding to cardiac muscarinic receptors is not a simple bimolecular reaction but likely involves a transition between at least two receptor–ligand configurations. These different receptor–ligand configurations may play a role in discriminating between G-protein conformations [21, 22]. Furthermore, this antagonist mediated transition of the receptor strongly depends on the integrity of the lipid environment and can be inhibited by PLA_2-induced phospholipid hydrolysis of sarcolemmal membranes.

Acknowledgements—This work was supported by the "Deutsche Forschungsgemeinschaft" within the "Sonderforschungsbereich 320", and the grants HL-21812 and HL-22135 from the National Institutes of Health.

APPENDIX

As outlined in the Discussion, the saturation kinetics of the apparent initial rates of [^{3}H]QNB-binding (see Fig. 3) exclude a simple bimolecular binding reaction, since a bimolecular binding mechanism would result in an initial association rate that linearly depends on the free concentration of the ligand. The following hypothetical reaction scheme for QNB-binding to cardiac muscarinic receptors therefore is assumed:

$$R + QNB \underset{k_{-1}}{\overset{k_1}{\rightleftharpoons}} R^*QNB \underset{k_{-2}}{\overset{k_2}{\rightleftharpoons}} R\text{-}QNB.$$
(step 1) (step 2)

According to Michaelis–Menten the free receptor R and the ligand QNB are in a rapid equilibrium with an unstable intermediate complex R*QNB, and the much slower conversion of R*QNB to the stable complex R-QNB is rate limiting (step 2).

Estimation of V_{max}, K_m, K_1 *and* k_2 *by analysis of the initial rate kinetics*

Ideally, under initial rate conditions the concentration of the final complex R-QNB is almost zero, and the dissociation of the final complex R-QNB (backwords reaction) can be neglected. Under these conditions, and under the assumption that the

conversion of the unstable intermediate complex R*QNB to the stable complex R-QNB is rate limiting (step 2), the initial association rate v_0 equals the product of the rate constant k_2 of the second step and the concentration of the intermediate complex R*QNB:

$$v_0 = k_2[\text{R*QNB}]. \quad (1)$$

Maximal velocity (V_{max}) of QNB-binding therefore can be obtained by extrapolating the concentration of QNB to infinite values (double reciprocal plot, Fig. 3B). Under these conditions all receptor binding sites are occupied by QNB, and R*QNB equals R_0 ($=B_{max}$).

Therefore, if [QNB] >> K_m:

$$[\text{R*QNB}] = [R_0]$$

(R_0 = total concentration of binding sites = B_{max})

$$v_0 = k_2[R_0] = V_{max}. \quad (1a)$$

As the maximal velocities (V_{max}) were obtained by the double reciprocal plots $1/v_0$ versus 1/QNB (Fig. 3B), and the concentration of R_0 can be estimated by measuring B_{max} (Fig. 4B), the rate constant k_2 can be calculated by the following equation:

$$k_2 = \frac{V_{max}}{[R_0]}. \quad (1b)$$

According to Michaelis–Menten v_0 is also described by:

$$v_0 = \frac{V_{max}[\text{QNB}]}{K_m + [\text{QNB}]}. \quad (2)$$

As $V_{max} = k_2[R_0]$ (see eqn 1a) eqn (2) can be rearranged as follows:

$$\frac{1}{v_0} = \frac{1}{k_2[R_0]} + \frac{K_m}{k_2[R_0]} \cdot \frac{1}{[\text{QNB}]}. \quad (2a)$$

$$y = b + m \cdot x \quad (2b)$$

Equation 2a describes straight lines corresponding to the double reciprocal plots shown in Fig. 3B. These linear curves are defined by the y-intercept $b = 1/k_2[R_0]$ and the slope $m = K_m/k_2[R_0]$. K_m depends on the rate constants of the hypothetical two step binding mechanism as follows:

$$K_m = \frac{k_{-1} + k_2}{k_1}. \quad (3)$$

Under the assumption that $k_2 << k_{-1}$ and k_1, the Michaelis constant K_m approximates to the value of the dissociation constant of the first reaction step K_1.

Therefore, if $k_2 << k_{-1}$:

$$K_m = \frac{k_{-1}}{k_1} = K_1. \quad (3a)$$

Estimation of k_{-2} *by analysis of the steady state kinetics*

As the ligand–receptor complex R-QNB is the endproduct of the binding reaction, steady state of the binding reaction is reached at binding equilibrium:

$$\text{R} \underset{k_{-1}}{\overset{k_1\text{QNB}}{\rightleftharpoons}} \text{R*QNB} \underset{k_{-2}}{\overset{k_2}{\rightleftharpoons}} \text{R-QNB}.$$

From this reaction model three receptor states, R, R*QNB and R-QNB can be differentiated. According to the King–Altman method of deriving steady state velocity equations [23, 24], the formation of any receptor state depends on the following interconversion patterns, which are the product of all rate constants and associated ligand concentrations that read along the lines leading to the receptor species in question (see above reaction model):

$$[\text{R}] \leftarrow k_{-1}k_{-2} \quad (4a)$$

$$[\text{R*QNB}] \leftarrow k_1k_{-2}[\text{QNB}] \quad (4b)$$

$$[\text{R-QNB}] \leftarrow k_1k_2[\text{QNB}] \quad (4c)$$

$$[R_0] \leftarrow (1a) + (1b) + (1c), \quad (4d)$$

where $[R_0]$ represents total receptor concentration.

The relation of the concentrations of the final product [R-QNB] and the total receptor $[R_0]$ then is:

$$\frac{[\text{R-QNB}]}{[R_0]} = \frac{k_1k_2[\text{QNB}]}{k_{-1}k_{-2} + k_1k_{-2}[\text{QNB}] + k_1k_2[\text{QNB}]} \quad (5)$$

$$[\text{R-QNB}] = \frac{k_1k_2[\text{QNB}][R_0]}{k_{-1}k_{-2} + [\text{QNB}]k_1(k_{-2} + k_2)} \quad (5a)$$

$$\frac{1}{[\text{R-QNB}]} = \frac{(k_{-2} + k_2) + k_{-1}k_{-2}/[\text{QNB}]k_1}{k_2[R_o]}. \quad (5b)$$

If $k_{-1}/k_1 = K_1$ (see eqn 3a), eqn (5b) can be rearranged:

$$\frac{1}{[\text{R-QNB}]} = \frac{k_{-2} + k_2}{k_2} \cdot \frac{1}{[R_0]} + \frac{k_{-2}K_1}{k_2[R_0]} \cdot \frac{1}{[\text{QNB}]} \quad (6)$$

$$y = b + m \cdot x. \quad (6a)$$

This is the equation of a straight line, as seen in Fig. 4B, where $(k_{-2} + k_2/k_2 \cdot [R_0])$ is the y-intercept (b) and $(k_{-2} \cdot K_1/k_2 \cdot [R_0])$ is the slope of the line (m). The intercept on the abscissa (x-intercept) then can be calculated as follows:

$$x = -b/m = -1/K_d \quad (6b)$$

$$K_d = \frac{m}{b} = \frac{k_{-2}K_1/k_2[R_0]}{(k_{-2} + k_2)/k_2[R_0]}. \quad (7)$$

The relation between the overall dissociation constant of QNB-binding K_d as measured by experiments in binding equilibrium, and the dissociation constant K_1 of the first step of the reaction as obtained from the kinetic experiments is now described as follows:

$$K_d = K_1 \frac{k_{-2}}{k_{-2} + k_2} \quad (7a)$$

$$k_{-2} = \frac{K_dk_2}{K_1 - K_d}. \quad (7b)$$

K_d is obtained from the experiments in binding equilibrium (x-intercept of Fig. 4B), K_1 is obtained from the kinetic measurements (x-intercept of Fig. 3B), and k_2 can be calculated as described above by eqn (1b).

REFERENCES

1. Aronstam RS, Abood LG and Baumgold J, Role of phospholipids in muscarinic binding by neutral membranes. *Biochem Pharmacol* **26**: 1689–1695, 1977.
2. Baron B and Kloog Y, Fatty acid incorporation increases the affinity of muscarinic cholinergic receptors for agonists. *Biochim Biophys Acta* **801**: 342–350, 1984.
3. Parthasarathy N, Pickard C and Aronstam RS, Influence of phospholipase C on muscarinic acetylcholine receptor binding in rat brain. *Neurochem Res* **9**: 709–717, 1984.
4. Moscona-Amir E, Henis YI, Yechiel E, Barenholz Y and Sokolovsky M, Role of lipids in age-related changes in the properties of muscarinic receptors in cultured rat heart myocytes. *Biochemistry* **25**: 8118–8124, 1986.
5. Rauch B, Colvin RA, Katz AM and Messineo FC, Effect of exogenous phospholipase A_2 treatment on cardiac muscarinic receptors of highly purified canine sarcolemmal vesicles. *J Mol Cell Cardiol* **19**: 569–580, 1986.
6. Rauch B, Colvin RA and Messineo FC, Inhibition of ^{3}H-quinuclidinyl benzylate binding to cardiac muscarinic receptor by long chain fatty acids can be attenuated by ligand occupation of the receptor. *J Mol Cell Cardiol* **21**: 495–506, 1989.
7. Chien KR, Reeves JP, Buja LM, Bonte F, Parkey RW and Willerson JT, Phospholipid alterations in canine ischemic myocardium. Temporal and topographical correlations with Tc-99m-PPi accumulation and an *in vitro* sarcolemmal Ca^{2+} permeability defect. *Circ Res* **48**: 711–719, 1981.
8. Hsueh W, Isakson PC and Needleman P, Hormone selective lipase activation in the isolated rabbit heart. *Prostaglandins* **13**: 1073–1091, 1977.
9. Shaikh NA and Downar E, Time course of changes in porcine myocardial phospholipid levels during ischemia. A reassessment of the lysolipid hypothesis. *Circ Res* **49**: 316–325, 1981.
10. Van der Vusse GJ, Roemen THM, Prinzen FW, Coumans WA and Reneman RS, Uptake and tissue content of fatty acids in dog myocardium under normoxic and ischemic conditions. *Circ Res* **50**: 538–546, 1982.
11. Corr PB, Gross RW and Sobel BE, Amphipathic metabolites and membrane dysfunction in ischemic myocardium. *Circ Res* **55**: 135–154, 1984.
12. Prinzen FW, van der Vusse GJ, Arts T, Roeman THM, Coumans WA and Reneman RS, Accumulation of nonesterified fatty acids in ischemic myocardium. *Am J Physiol* **247**: H264–H272, 1984.
13. Katz AM and Messineo FC, Lipid-membrane interactions and the pathogenesis of ischemic damage in the myocardium. *Circ Res* **48**: 1–16, 1981.
14. Galper JB, Klein W and Catterall WA, Muscarinic acetylcholine receptors in developing chick heart. *J Biol Chem* **252**: 8692–8699, 1977.
15. Schimerlik MI and Searles RP, Ligand interactions with membrane-bound porcine atrial muscarinic receptor(s). *Biochemistry* **19**: 3407–3413, 1980.
16. Jones LR, Maddock SW and Besch HR Jr, Unmasking effect of alamethicin on the (Na^+,K^+)-ATPase, beta-adrenergic receptor-coupled adenylate cyclase, and cAMP dependent protein kinase activities of cardiac sarcolemmal vesicles. *J Biol Chem* **255**: 9971–9980, 1980.
17. Colvin RA, Ashavaid TF and Herbette L, Structure–function studies of canine cardiac sarcolemmal membranes. I. Estimation of receptor site densities. *Biochim Biophys Acta* **812**: 601–608, 1985.
18. Lowry OH, Rosenbrough NJ, Farr AL and Randall AJ, Protein measurement with the Folin phenol reagent. *J Biol Chem* **193**: 265–275, 1951.
19. Roelofsen B and op den Kamp J, Chemical and enzymatic localization of phospholipids in biological membranes. In: *Techniques in Lipid and Membrane Biochemistry*. Elsevier Scientific Publishers Ltd, New York, 1982.
20. Rauch B, von Chak D and Hasselbach W, Phosphorylation by inorganic phosphate of sarcoplasmic membranes. *Z Naturforsch* **32c**: 828–834, 1977.
21. Costa T and Herz A, Antagonists with negative intrinsinc activity at delta opioid receptors coupled to GTP-binding proteins. *Proc Natl Acad Sci USA* **86**: 7321–7325, 1989.
22. Taylor CW, The role of G proteins in transmembrane signalling. *Biochem J* **272**: 1–13, 1990.
23. Segel IH, Enzyme Kinetics. In: *Behaviour and Analysis of Rapid Equilibrium and Steady State Enzyme Systems*. pp. 170–176. John Wiley & Sons, New York, 1975.
24. King EL and Altman C, A schematic method of deriving the rate laws for enzyme-catalyzed reactions. *J Physiol Chem* **60**: 1375–1378, 1956.